



Tunable self-biased magnetoelectric response in homogenous laminates

Yuan Zhou, Su Chul Yang, Daniel J. Apo, Deepam Maurya, and Shashank Priya

Citation: [Applied Physics Letters](#) **101**, 232905 (2012); doi: 10.1063/1.4769365

View online: <http://dx.doi.org/10.1063/1.4769365>

View Table of Contents: <http://scitation.aip.org/content/aip/journal/apl/101/23?ver=pdfcov>

Published by the [AIP Publishing](#)



Re-register for Table of Content Alerts

Create a profile.



Sign up today!



Tunable self-biased magnetoelectric response in homogenous laminates

Yuan Zhou,^{a)} Su Chul Yang, Daniel J. Apo, Deepam Maurya, and Shashank Priya^{a)}

Bio-inspired Materials and Devices Laboratory (BMDL), Center for Energy Harvesting Materials and Systems (CEHMS), Virginia Tech, Virginia 24061, USA

(Received 16 August 2012; accepted 15 November 2012; published online 6 December 2012)

In this study, we demonstrate self-biased magnetoelectric effect in homogenous two-phase magnetostrictive-piezoelectric laminates. Our results illustrate the method for tuning the magnitude of self-bias effect and provide understanding behind the hysteretic changes. We model this phenomenon by considering the magnetization hysteresis with shape-induced demagnetization effect. The self-biased response was found to be directly related to the nature of magnetization and can be tuned by variation in demagnetization state and the resultant differential magnetic flux distribution. These results present significant advancement toward development of AC magnetic field sensor and magnetoelectric composite based on-chip devices by eliminating the need for DC bias. © 2012 American Institute of Physics. [<http://dx.doi.org/10.1063/1.4769365>]

Magnetoelectric (ME) composites are promising for applications in magnetic field sensors, filters, transformers, and memory devices.^{1,2} The composite structures consisting of piezoelectric and magnetostrictive phases possess stronger ME coupling in comparison to that of single phase materials.^{1,2} In direct ME effect, the measured coupling coefficient is the field conversion ratio between the applied AC magnetic field (H_{ac}) and the induced AC electric field (E_{ac}), $\alpha_{ME} = \delta E_{ac} / \delta H_{ac}$, which is directly related to effectiveness of elastic coupling between two phases and piezomagnetic coefficient ($q = d\lambda/dH$, λ : magnetostriction) of magnetostrictive phase. The dependence of α_{ME} on q indicates the requirement for additional DC magnetic bias (H_{bias}).³ Depending upon the composition and shape of magnetostrictive phase, one can tune the magnitude of optimum DC bias ranging from 5 Oe to 6.8 kOe.¹⁻³ However, these composites then require permanent magnet or coil as DC magnetic bias source, which hinders their implementation on thick or thin film platform. In this paper, we present a homogenous two-phase magnetostrictive (ferromagnetic)-piezoelectric composite structure with large tunable α_{ME} in the absence of DC magnetic field. This structure opens the possibility for designing MEMS-scalable energy harvesting components.

Recent studies have shown the possibility of achieving self-biased α_{ME} by combining flexural deformation and ferromagnetic composition graded structure in the case of bulk composite.⁴⁻⁹ Alternative approaches have been suggested for the case of thin films that rely on magnetic field-dependence of resonant frequency and angular dependence of exchange bias field.^{10,11} This phenomenon is promising for applications such as magnetic field sensor, core-free magnetic flux control device, and electrically controlled magnetic memory devices.^{5,12,13} The focus of prior studies on bulk structure has been mainly on understanding the nature of self-bias effect in terms of grading of ferromagnetic composition and bending resonance.^{7,9,14} However, these structure present another level of practical difficulty for on-chip components as synthesis process has to account for hetero-

genous graded structure or two-phase magnetic layers along with flexural deformation. Furthermore, the self-biased effect due to the grading induced build-in field lacks the feasibility for controllable tunability. Thus, even though these structures are intriguing, their implementation for realization of on-chip components and tunable devices will be limited.

In addressing this issue, we provide a significant breakthrough in this paper and demonstrate self-biased response in homogeneous ferromagnetic system. We further model this phenomenon and its tunable characteristics by considering the nature of ferromagnetic material and shape-induced demagnetization effect.

0.8[Pb(Zr_{0.52}Ti_{0.48})O₃]-0.2[Pb(Zn_{1/3}Nb_{2/3})O₃] + 2 mol. %MnO₂ (PMT) were synthesized by conventional mixed oxide method and shaped into plates of dimension 10 × 5 × 0.3 mm³. After poling, 0.15-mm-thick Metglas sheet (4 layers, 2605SA1, Metglas Inc., USA) or “*n*” layers of 0.15-mm-thick Ni foil (McMaster -Carr, USA) with different lateral dimension were laminated on the PMT plate by using epoxy resin (West System, USA) to form the bilayer laminates. The ME effect was measured in L-T mode (longitudinally magnetized and transversely poled) configuration with sample located in the center of the Helmholtz coil (H_{ac}) which itself was located in the center of large electromagnet (H_{dc}). The induced voltage was monitored using a lock-in amplifier. The magnetization of the ferromagnetic layer was measured by using vibrating sample magnetometer (VSM 7340, Lake Shore Cryotronics). The magnetic domain structure was observed by magnetic force microscopy (Dimension Icon AFM, Bruker) in the tapping-lift mode. Magnetostriction was measured by using the strain gauge and Wheatstone bridge. Impedance spectrum of the laminate was measured by an LCR meter (HP4194A, USA).

We characterized the magnetoelectric properties of the Ni-PMT and Metglas-PMT bilayer laminates as a function of DC magnetic field H_{dc} at 1 kHz with $H_{ac} = 1$ Oe, as shown in Figure 1. The α_{ME} of Metglas-PMT bilayer structure shows non-hysteretic cyclic response as a function of H_{dc} , with maximum occurring at 68 Oe. Most of the ferromagnetic materials exhibit zero piezomagnetic coefficient when $H_{dc} = 0$ and consequently negligible α_{ME} near zero bias. In

^{a)} Authors to whom correspondence should be addressed. Electronic addresses: spriya@vt.edu and yzhou6@vt.edu.

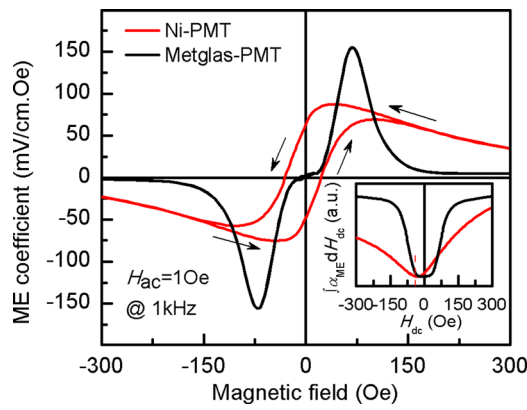


FIG. 1. ME coefficients (α_{ME}) of Ni-PMT and Metglas-PMT bilayer laminates as function of DC magnetic field (H_{dc}). Inset shows integral values of ME coefficient with respect to magnetic field.

comparison, we noticed that the α_{ME} of Ni-PMT bilayer shows a hysteretic behavior during H_{dc} sweep (anticlockwise direction), with a large response of $\sim \pm 63.3 \text{ mV cm}^{-1} \text{ Oe}^{-1}$ at zero DC magnetic bias, $\sim 72.5\%$ of its maximum α_{ME} value ($87.3 \text{ mV cm}^{-1} \text{ Oe}^{-1}$). It should be further noted here that this laminate system does not have magnetic gradient structure. Considering the intrinsic relationship for α_{ME} of composites $= \left| \frac{\partial T}{\partial S} \times \frac{\partial D}{\partial T} \times \frac{\partial E}{\partial D} \right| \times \frac{\partial S}{\partial H}$, where first part is non-magnetic factor, one can derive $\alpha_{ME} \propto \frac{\partial S}{\partial H} = \frac{d\lambda}{dH} = q$. We estimated the effective λ by integrating α_{ME} with respect to the H_{dc} as shown in the inset of Fig. 1. Metglas-PMT shows symmetrical λ -behavior with respect to H_{dc} while the tendency of λ for Ni-PMT was asymmetric. Thus, the hysteretic behavior is related to the nature of magnetostrictive materials.

In order to further elucidate the reason for self-biased hysteretic behavior, we measured magnetization (M) of Ni and Metglas as a function of H_{dc} in longitudinal direction (in-plane) as shown in Fig. 2(a). The hysteretic behavior of magnetization for Ni in the range of ± 300 Oe can be immediately noticed in comparison with Metglas. This phenomenon could be attributed to the change in the structure of magnetic domains in both materials. Magnetic force microscopy (MFM) was conducted on Ni and Metglas surface to understand the differences in magnetic domain structure as shown in the inset image of Fig. 2(a). Nanosized striped domains in Metglas can be easily aligned in the direction of applied H-field exhibiting small coercive field and high reversibility. The absence of grain boundary in amorphous metglas contributes towards the lower coercive field. However, nickel foil was found to possess macrosized domains with long range ordering which resulted in larger coercive field than that of Metglas. Once the magnetic domains were reoriented, it required higher field to achieve the random state resulting in larger hysteresis in the magnetization curve. This difference in the hysteretic behavior originating from the differences in the crystallinity and domain structure is reflected in the magnetization response. We can also correlate this magnetization behavior with magnetostriction through the relation given as^{15,16}

$$\varphi \sim \frac{3\lambda\sigma}{(K + 2\pi M^2)} \quad \text{or} \quad \lambda \propto M^2, \quad (1)$$

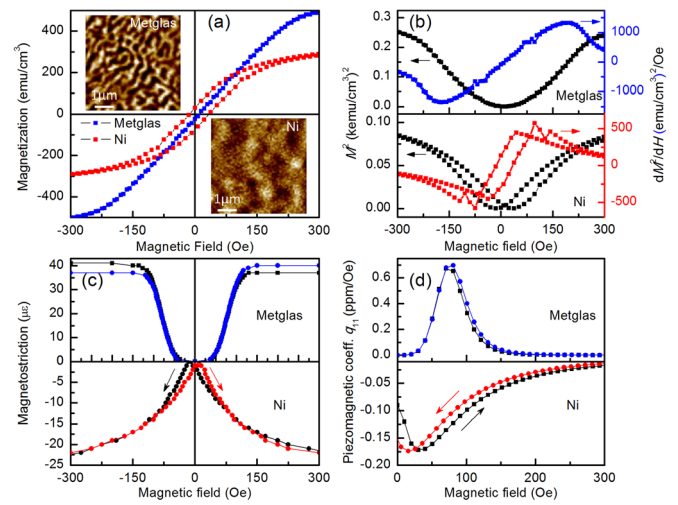


FIG. 2. (a) Magnetization-magnetic field (M - H) response. Inset shows magnetic domain images on the surface of Metglas and Ni scanned by MFM; (b) square magnetization-magnetic field (M^2 - H) and differential of square magnetization-magnetic field $[(dM^2/dH)-H]$; (c) DC magnetic field (H_{dc}) dependence of the magnetostriction (λ_{11}); (d) DC magnetic field (H_{dc}) dependence of piezomagnetic coefficients (q_{11}) for Ni and Metglas.

where φ is the angle of magnetic moments, K and σ are the anisotropy constant and stress, respectively. As shown in Fig. 2(b), M^2 - H curves indicate that there was no obvious hysteresis in Metglas, while large hysteresis occurs in Ni. Using Eq. (1), and considering $\alpha_{ME} \propto q = d\lambda/dH$, we can obtain the relationship $\alpha_{ME} \propto dM^2/dH$. Hence, the magnitude of dM^2/dH can be used to predict the behavior of ME composites with respect to applied magnetic field. It was found that the (dM^2/dH) - H behavior of Metglas and Ni based laminates matched well with experimental data shown in Fig. 1. Note that Fig. 2(b) shows only the qualitative nature of effective λ , q behavior of magnetostrictive layer and not quantitative values. Therefore, we believe that difference in the domain and microstructure of Metglas and Ni as observed by MFM and resultant different behavior of M^2 - H and (dM^2/dH) - H behavior are the origin of the self-biased ME response. Based on this hypothesis, we measured the in-plane magnetostriction (λ_{11}) as a function of applied H_{dc} . It can be clearly seen from Fig. 2(c) that the behavior of λ_{11} was similar to that of M^2 - H curve. Using λ_{11} curves, we obtained the q_{11} curves as shown in Fig. 2(d). These measurements confirmed that Ni has hysteretic behavior in comparison to Metglas.

From the point of view of functional ME devices, it is important to control the magnitude of self-biased ME voltage coefficient. Thus, we investigated the effect of geometry on tunability of self-biased response. First, N layers (1, 2, 4) of Ni sheets with same dimension ($10 \times 5 \times 0.15 \text{ mm}^3$) were laminated on to the PMT plates. As shown in Fig. 3(a), the variation in a_{ME} exhibited similar trend as function of H_{dc} under varying thickness ratio ($t_{m/p}$). In all cases, a_{ME} shows hysteretic loop with anticlockwise direction sweep. The values of increasing-field maximum (a_{H1}) and decreasing-field maximum (a_{H2}) with thicker Ni layer were notably higher than that for thinner ones, while also requiring larger magnetic biases (increasing-field optimum, $H1$ and decreasing-field optimum, $H2$). The magnitude of self-biased point (a_{H0}) slightly

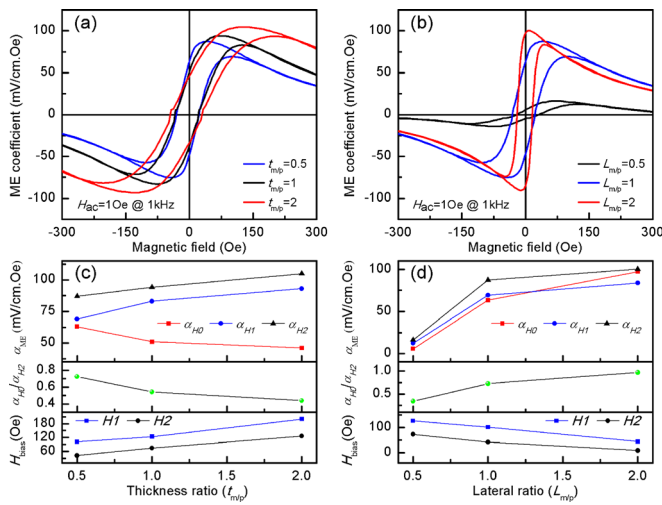


FIG. 3. (a) ME voltage coefficient (α_{ME}) of Ni-PMT laminates with varied thickness ratio; (b) ME voltage coefficient (α_{ME}) of Ni-PMT laminates with varied lateral dimension; (c) ME voltage coefficient values of self-biased point (a_{H0}), increase-field maximum (a_{H1} , $H1$), decrease-field maximum (a_{H2} , $H2$) and self-bias coefficient (a_{H0}/a_{H2}) as function of thickness ratio; (d) ME voltage coefficient values of self-biased point (a_{H0}), increase-field maximum (a_{H1} , $H1$), decrease-field maximum (a_{H2} , $H2$) and self-bias coefficient (a_{H0}/a_{H2}) as function of lateral dimension.

decreases as thickness ratio increases as shown in Fig. 3(c). The maximum self-biased ME response was achieved at $t_{m/p} = 0.5$. Next, we fixed the thickness ratio at $t_{m/p} = 0.5$ and varied the lateral dimension as shown in Fig. 3(b). It can be seen in this figure that the magnitude of $a_{H0} \sim H2$ increased dramatically as lateral ratio ($L_{m/p}$) increased from 0.5 to 2. Notably, a giant self-bias coefficient (a_{H0}/a_{H2}) of 97% was achieved at $L_{m/p} = 2$, compared to 34.4% and 72.5% at $L_{m/p} = 0.5$ and 1, as shown in Fig. 3(d). The hysteresis loop was tilted toward y-axis as the optimum magnetic bias ($H1$ and $H2$) decreased. Based upon these results, we can obtain and tune the self-bias coefficient by selecting suitable magnetic phase with proper geometry and dimension.

The ME response of Ni-PMT laminate can be explained by taking into account the constitutive piezoelectric and piezomagnetic behavior. Figure of merit for the ME composite in L-T mode is given as^{1,17}

$$\alpha_{E,31} = \frac{dE_3}{dH_1} = \frac{nq_{11}g_{31}}{nS_{11}^p(1 - k_{31}^2) + (1 - n)S_{11}^m}, \quad (2)$$

where E_k and H_k are vector components of the electric and magnetic field, n is the volume fraction of magnetic phase $n = \frac{m_v}{(p_v + m_v)}$, v denotes the volume, q_{11} is piezomagnetic coefficient, g_{31} is piezoelectric voltage coefficient, S_{ij} is compliance coefficient, and k_{31} is electromechanical coupling coefficient. The superscripts "m" and "p" represent the magnetostrictive and piezoelectric phase, respectively. This relationship clearly reflects the important role of material parameters of piezoelectric phase (g_{31} , S_{11}^p) and magnetostrictive phase (q_{11} , S_{11}^m) towards achieving large magneto-electric response. At specific bias magnetic field, the magnitude of piezomagnetic coefficient is fixed. For a given piezoelectric phase, the ME voltage coefficient in the laminated composite is mainly determined by the magnetic phase ratio n , $\alpha_{ME} \propto n$. By fixing the piezoelectric layer dimen-

sions, as we increase the magnetic phase thickness ratio or lateral dimension, the volume ratio n will increase. In this study, for volume ratio of less than ~ 0.67 , the maximum α_{ME} (a_{H1} and a_{H2}) increased with increasing n at an optimum bias field, which is consistent with the prediction based upon Eq. (2). However under zero-bias condition, we found that the value of α_{ME} (a_{H0}) decreased with increasing thickness ratio, which is contradictory to the prediction by Eq. (2). Moreover, there are some questions in Fig. 3 that need to be addressed and we list them here: (i) For same magnetic phase volume ratio, why α_{ME} under zero-bias condition shows different value and tendency as a function of thickness and lateral dimension? and (ii) Why H_{bias} shifts back and forth as a function of sample shape and size?

To better explain above questions and the tunable nature of self-biased ME response, the size-induced demagnetization effect was taken into consideration.¹⁸ For ferromagnetic materials, the demagnetization field is directly proportional to demagnetization factor (N_d), $H_d = MN_d$ (M is the magnetization), where N_d is dependent on the dimension and geometry. Thus, the internal effective magnetic field (H_{eff}) in the magnetic phase can be written as

$$H_{eff} = H_{bias} - H_d, \quad (3)$$

where H_{bias} is the induced external magnetic field. For a finite, non-spherical ferromagnet, a good approximation to N_d can be found from the general ellipsoid solution of Osborn¹⁹

$$N_d \approx (wt/l^2)(\ln(4l/(w+t)) - 1), \quad (4)$$

where l is the length, w is the width and t is the thickness. Fig. 4(a) shows the variation of N_d as a function of magnetic phase ratio. Clearly, a smaller N_d will result in a lower H_d , and thus a more effective H_{eff} . Therefore, in order to achieve same magnitude of H_{eff} , one needs to apply larger H_{bias} when H_d is larger and vice-versa, which is also compatible with experimental data shown in Figs. 3(c) and 3(d). However, it is difficult to determine how the magnetization of a material varies with the external magnetic field due to shape/location induced anisotropy. Therefore using Eq. (3) and considering the magnetization relationship $B = \mu_0(H + M)$, the effective magnetic induction can be found as

$$B_{eff} = \mu_0(H_{eff} + M) = \mu_0(H_{bias} + M) - \mu_0MN_d. \quad (5)$$

Again, it can be seen that a smaller N_d will result in a stronger B_{eff} . Further, it has been shown that high magnetic flux concentration in magnetic phase has positive effect on the magneto-electric response of ME laminates.^{20,21} Thus, there should be correlation between the tunable feature of self-biased ME response and the variation of magnetic flux concentration of magnetic phase with geometry.

To find this correlation, finite element simulation using ANSYS MULTIPHYSICS (version 14) was conducted for Ni sheets with dimensions similar to those used in the experiments. The magnetostatic modeling assumed the nickel is in air and has relative permeability of 600 and coercive force (in the axial length direction) of 0.7 Oe.²² A parallel flux boundary condition was applied around the magnet. For each simulation, the magnet was meshed between 10,000 and 100,000

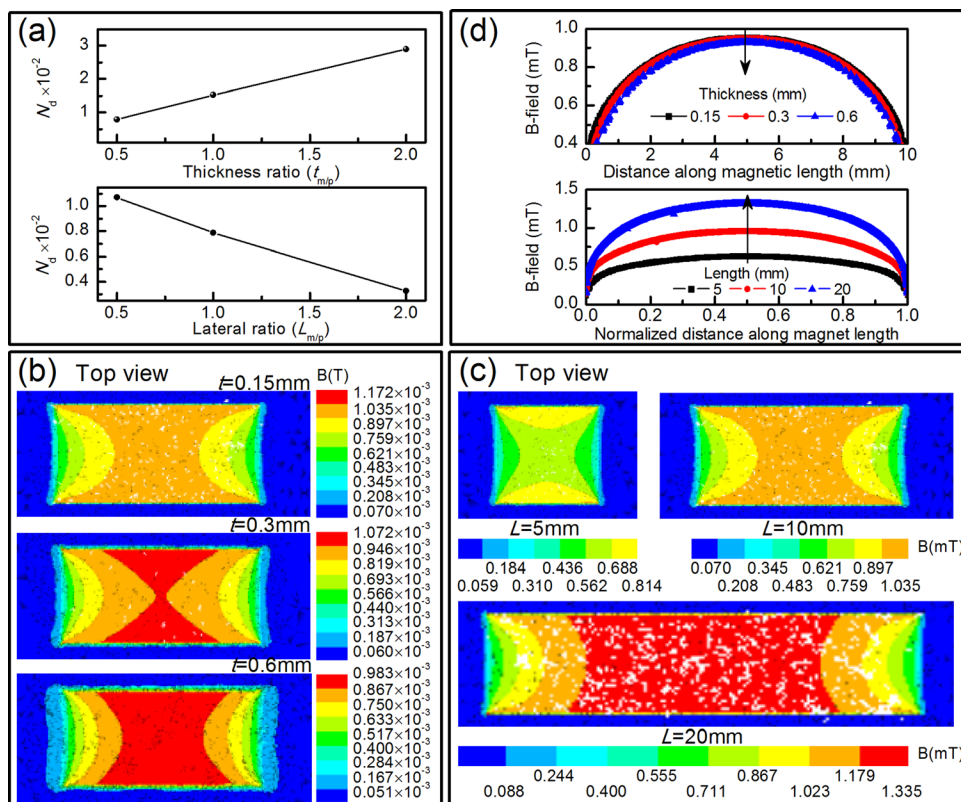


FIG. 4. (a) Demagnetization factor variation as function of sample thickness/lateral ratio; (b) in-plane magnetic field strength along the center plane of Ni sheets for variation in thickness, with fixed in-plane size, in response to zero DC bias field, as simulated by ANSYS; (c) in-plane magnetic field strength along the center plane of Ni sheets for variation in length, with fixed thickness, in response to zero DC bias field; (d) line scan traces of magnetic flux density along the axial centerline of Ni for variation in thickness and length.

points and the simulations were within 0.01% accuracy. Fig. 4(b) shows that laminates with thicker magnetic phase sheet possess weaker magnetic induction, which will further result in decrease in ME coupling. The laminates with longer magnetic phase sheets produced a much stronger magnetic induction as shown in Fig. 4(c), and a resultant large increase in ME coupling. By using the results shown in Figs. 4(b) and 4(c), we can further compute line scans of the magnitude of magnetic flux density along the axial center-line of the Ni sheets with different geometry in Fig. 4(d), which is also compatible with the results obtained from Fig. 4(a) and Eq. (5). These results match well with the experimental data in Fig. 3 and imply that tunable self-biased ME effect was obtained due to magnetic flux concentration variation occurring due to size-induced demagnetization effect.

To achieve the best ME performance, working at electromechanical resonance of piezoelectric phase is necessary.²³ Therefore, we investigated the frequency dependence of self-biased ME response in optimized Ni-PMT laminate ($L_{m/p}=2$). Fig. 5(a) shows the impedance spectrum and ME response under varying H_{dc} condition. The frequency dependence of a_{ME} shows resonance peaks corresponding to bending modes. It can be noticed that even though there is no H_{dc} , self-biased ME response follows the same trend and has similar magnitude of voltage coefficient as to that of sample in biased conditions. Fig. 5(b) shows the effect of magnetic field strength (H_{ac}) under zero bias ($H_{dc}=0$ Oe) condition at different frequency. Linear increase in ME voltage was observed with increasing AC voltage on Helmholtz coil (H_{ac}). Further increase in the linear slope was achieved by working at resonant mode. We obtained a_{ME} values of $585.7 \text{ mV cm}^{-1} \text{ Oe}^{-1}$ at 15.5 kHz and $91.2 \text{ mV cm}^{-1} \text{ Oe}^{-1}$ at 1 kHz given by the slope which matches well with the measured value in Fig. 5(a). These results illustrate that

under zero DC bias condition, high ME response can be sustained in homogenous ME laminates.

The magnitude of the ME coefficient can be further increased by developing the flexural resonant structure mounted in cantilever configuration. We fabricated a ME

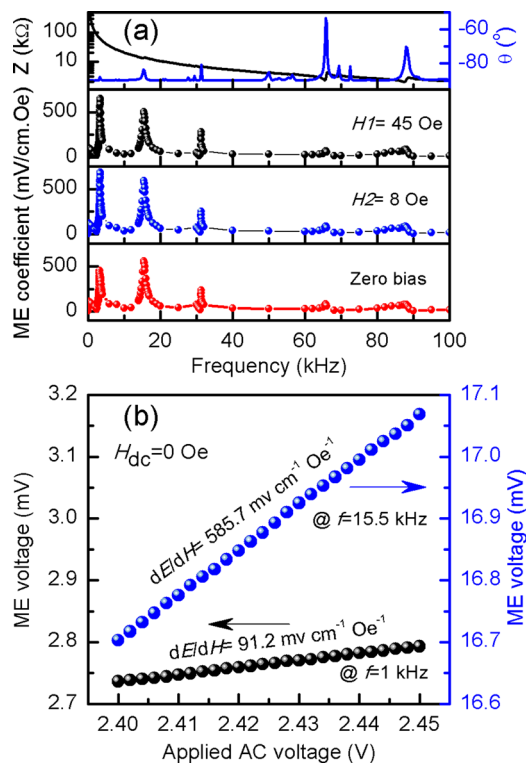


FIG. 5. (a) Impedance and phase spectrum and its ME voltage coefficient as function of applied AC frequency; (b) source free ($H_{dc}=0$ Oe) ME voltage output of Ni-PMT laminate measured at 1 kHz and 15.5 kHz under various applied AC voltage on Helmholtz coil (H_{ac}).

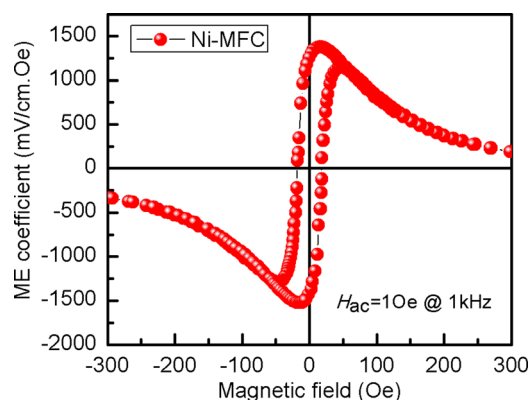


FIG. 6. ME coefficients of Ni-MFC bilayer laminates as a function of DC magnetic field.

composite operating in L-L mode consisting of a MFC (dimension $40 \times 10 \text{ mm}^2$, Model: M-4010-P1, Smart Material Corp., USA) and 1 layer of 0.15-mm-thick Ni foil with dimension of $80 \times 10 \text{ mm}^2$. The ME effect was measured in L-L mode configuration and the result is shown in Fig. 6. The α_{ME} of Ni-MFC bilayer shows a hysteretic behavior during H_{dc} sweep (anticlockwise direction) with a large response of $\sim 1254 \text{ mV cm}^{-1} \text{ Oe}^{-1}$ at zero DC magnetic bias, $\sim 90.8\%$ of its maximum α_{ME} value ($1381 \text{ mV cm}^{-1} \text{ Oe}^{-1}$). Please note that these measurements were conducted in off-resonance condition at 1 kHz.

In conclusion, we demonstrate that the homogenous two-phase ferromagnetic-piezoelectric laminate Ni/PMT composite exhibits large self-biased ME response. We achieved tunable self-biased response in bilayer composite structure with homogeneous ferromagnetic layer which has great advantage in integration with MEMS-scale devices.

The authors gratefully acknowledge the financial support from AFOSR through Young Investigator Program. The authors also thank the Office of Naval Research for support-

ing the research (Y. Zhou) through Center for Energy Harvesting Materials and Systems.

- ¹C. W. Nan, M. I. Bichurin, S. X. Dong, D. Viehland, and G. Srinivasan, *J. Appl. Phys.* **103**, 031101 (2008).
- ²G. Srinivasan, *Annu. Rev. Mater. Res.* **40**, 153 (2010).
- ³S. X. Dong, J. Y. Zhai, J. F. Li, and D. Viehland, *Appl. Phys. Lett.* **89**, 252904 (2006).
- ⁴S. C. Yang, C. S. Park, K. H. Cho, and S. Priya, *J. Appl. Phys.* **108**, 093706 (2010).
- ⁵S. C. Yang, K. H. Cho, C. S. Park, and S. Priya, *Appl. Phys. Lett.* **99**, 202904 (2011).
- ⁶S. C. Yang, C. W. Ahn, K. H. Cho, and S. Priya, *J. Am. Ceram. Soc.* **94**, 3889 (2011).
- ⁷S. K. Mandal, G. Sreenivasulu, V. M. Petrov, and G. Srinivasan, *Phys. Rev. B* **84**, 014432 (2011).
- ⁸S. K. Mandal, G. Sreenivasulu, V. M. Petrov, and G. Srinivasan, *Appl. Phys. Lett.* **96**, 192502 (2010).
- ⁹U. Laletin, G. Sreenivasulu, V. M. Petrov, T. Garg, A. R. Kulkarni, N. Venkataramani, and G. Srinivasan, *Phys. Rev. B* **85**, 104404 (2012).
- ¹⁰E. Lage, C. Kirchof, V. Hrkac, L. Kienle, R. Jahns, R. Knöchel, E. Quandt, and D. Meyners, *Nature Mater.* **11**, 523 (2012).
- ¹¹T. D. Onuta, Y. Wang, C. J. Long, and I. Takeuchi, *Appl. Phys. Lett.* **99**, 203506 (2011).
- ¹²Y. M. Jia, S. W. Or, H. L. W. Chan, X. Y. Zhao, and H. S. Luo, *Appl. Phys. Lett.* **88**, 242902 (2006).
- ¹³Y. J. Wang, F. F. Wang, S. W. Or, H. L. W. Chan, X. Y. Zhao, and H. S. Luo, *Appl. Phys. Lett.* **93**, 113503 (2008).
- ¹⁴G. Sreenivasulu, S. K. Mandal, S. Bandekar, V. M. Petrov, and G. Srinivasan, *Phys. Rev. B* **84**, 144426 (2011).
- ¹⁵V. K. Vlasko-Vlasov, Y. K. Lin, D. J. Miller, U. Welp, G. W. Crabtree, and V. I. Nikitenko, *Phys. Rev. Lett.* **84**, 2239 (2000).
- ¹⁶S. Ito, K. Aso, Y. Makino, and S. Uedaira, *Appl. Phys. Lett.* **37**, 665 (1980).
- ¹⁷S. X. Dong and J. Y. Zhai, *Chin. Sci. Bull.* **53**, 2113 (2008).
- ¹⁸C. M. Van der Burgt, *Philips Res. Rep.* **8**, 91 (1953).
- ¹⁹J. A. Osborn, *Phys. Rev.* **67**, 351 (1945).
- ²⁰Z. Fang, S. G. Lu, F. Li, S. Datta, Q. M. Zhang, and M. El Tahchi, *Appl. Phys. Lett.* **95**, 112903 (2009).
- ²¹J. Q. Gao, D. Gray, Y. Shen, J. F. Li, and D. Viehland, *Appl. Phys. Lett.* **99**, 153502 (2011).
- ²²W. F. Brown, *Handbook of Chemistry and Physics*, edited by Condon and Odishaw (McGraw-Hill, New York, 1958), Chap. 8.
- ²³M. I. Bichurin, D. A. Filippov, V. M. Petrov, V. M. Laletsin, N. Paddubnaya, and G. Srinivasan, *Phys. Rev. B* **68**, 132408 (2003).